Title:

Calcification by Juvenile Corals under Heterotrophy and Elevated CO_2

Authors:

E. J. Drenkard[1], A. L. Cohen[2], D. C. McCorkle[2], S. J. de Putron[3], V. R. Starczak[2], A. E. Zicht[4]

Institutions:

[1]Woods Hole Oceanographic Institution Joint Program in Oceanography, Massachusetts Institute of Technology, Cambridge, MA 02139, USA
[2]Woods Hole Oceanographic Institution, Woods Hole, MA, 02543
[3]Bermuda Institute of Ocean Sciences, St. George's GE 01, Bermuda
[4]Oberlin College, Oberlin, OH 44074 (Currently at Rutgers University, Institute of Marine and Coastal Sciences, New Brunswick, NJ 08901, USA)

Corresponding Authors:

Liz Drenkard
266 Woods Hole Rd.
Clark 120A (MS# 23)
Woods Hole, MA 02543-1050
Phone: 1-508-289-3831
Fax: 1-508-457-2175
Email: edrenkard@whoi.edu

Anne Cohen
266 Woods Hole Rd.
Clark 118 (MS# 23)
Woods Hole, MA 02543-1050
Phone: 1-508-289-2958
Fax: 1-508-457-2183
Email: acohen@whoi.edu

Keywords:

Climate Change; Ocean Acidification; Coral Reefs; Coral Calcification; heterotrophy; energetics

Abstract

Ocean acidification (OA) threatens the existence of coral reefs by slowing the rate of calcium carbonate ($CaCO_3$) production of framework-building corals thus reducing the amount of $CaCO_3$ the reef can produce to counteract natural dissolution. Some evidence exists to suggest that elevated levels of dissolved inorganic nutrients can reduce the impact of OA on coral calcification. Here, we investigated the potential for enhanced energetic status of juvenile corals, achieved via heterotrophic feeding, to modulate the negative impact of OA on calcification. Larvae of the common Atlantic golf ball coral, Favia fragum, were collected and reared for 3 weeks under ambient (421 μatm) or significantly elevated (1,311 μatm) CO_2 conditions. The metamorphosed, zooxanthellate spat were either fed brine shrimp (i.e., received nutrition from photosynthesis plus heterotrophy) or not fed (i.e., primarily autotrophic). Regardless of CO_2 condition, the skeletons of fed corals exhibited accelerated development of septal cycles and were larger than those of unfed corals. At each CO_2 level, fed corals accreted more $CaCO_3$ than unfed corals, and fed corals reared under 1,311 μatm CO_2 accreted as much $CaCO_3$ as unfed corals reared under ambient CO_2. However, feeding did not alter the sensitivity of calcification to increased CO_2; Δcalcification/ΔΩ was comparable for fed and unfed corals. Our results suggest that calcification rates of nutritionally replete juvenile corals will decline as OA intensifies over the course of this century. Critically, however, such corals could maintain higher rates of skeletal growth and $CaCO_3$ production under OA than those in nutritionally limited environments.

Introduction

The ocean has absorbed 25–30 % of the CO_2 emitted by human activities, driving a 0.1 unit decline in surface ocean pH and a 30 % decrease in carbonate ion concentration ($[CO_3^{2-}]$), a process known as ocean acidification (OA) (Caldeira and Wickett 2003; Feely et al. 2004). Scleractinian corals build skeletons of aragonite, a polymorph of calcium carbonate ($CaCO_3$), and rely on carbonate ions for calcification (Marubini and Atkinson 1999; Silverman et al. 2007; de Putron et al. 2011). The aragonite saturation state (Ωar, $[Ca^{2+}][CO_3^{2-}]/K_{sp(arag)}$) of seawater reflects the thermodynamic tendency for $CaCO_3$ to form (Ω > 1) or dissolve (Ω < 1). Although the tropical oceans where most coral reefs are located are not likely to become under saturated with respect to aragonite (Ω□□<1) during this century, most experimental studies show that skeletal growth and $CaCO_3$ production by corals are negatively impacted by OA long before aragonite under saturation is reached. On the ecosystem scale, the relative rates of $CaCO_3$ production versus dissolution are critical for coral reefs. If rates of production fall below natural rates of erosion and dissolution, reefs will shift from net accreting to net dissolving structures (Orr et al. 2005; Silverman et al. 2009), diminishing their capacity to provide habitats for marine organisms and to function as effective barriers against waves and tsunamis. Using coral reef community calcification data from the Gulf of Aqaba, Silverman et al. (2009) predicted a global-scale shift from net accreting to net dissolving reefs within the next 60 yrs.

The impact of Ωar on calcification by reef organisms has been explored largely in laboratory manipulation experiments, although a handful of in situ datasets provide key insights into the sensitivity of ecosystem-scale calcification to rising CO_2 levels (e.g., Silverman et al. 2007; Shamberger et al. 2011). In general, these studies have shown that both coral and coral reef calcification decline with decreasing Ωar (reviewed in Langdon et al. 2000; Hoegh-Guldberg et al.

2007; Fabry et al. 2008; Doney et al. 2009; Pandolfi et al. 2011), but there is considerable variability among populations, species, and studies in the calcification response or sensitivity at a given Ωar (summarized in Pandolfi et al. 2011). There is also variability in the absolute rates of calcification among different corals and coral reefs at the same Ωar (Shamberger et al. 2011). For example, flume incubations of Hawaiian *Porites compressa* and *Montipora verrucosa* show a positive, linear relationship between Ωar and calcification rate (mmol $CaCO_3$ m^{-2} h^{-1}) (Langdon and Atkinson 2005). However, de Putron et al. (2011) reported a nonlinear relationship between Ωar and calcification by Bermudan *Favia fragum* and *Porites asteroides* over a similar range of Ωar, while Ries et al. (2010) found that *Oculina sp.* responded only at a treatment pCO_2 of 2,800 ppm (Ωar < 1) and not at values of 900 ppm and below. On the scale of coral reef communities, different reef ecosystems at the same Ωar exhibit significant differences in the rate of net reef calcification. For example, the average net calcification rate of a Red Sea reef was reported as 54.5 mmol CaCO3 m^{-2} h^{-1} at an average Ωar of 3.9 (Silverman et al. 2007), whereas average net calcification rate of the Kaneohe Bay barrier reef on Hawaii was significantly higher (264.2 mmol $CaCO_3$ m^{-2} h^{-1}) despite a significantly lower average Ωar (2.9) (Shamberger et al. 2011). Multiple environmental and biological factors that influence biogenic calcification on a coral reef could be invoked to explain the variability, but few have been directly tested.

Here, we conducted an experiment in which the nutritional status of zooxanthellate (photosynthesizing) juvenile corals, that were reared under very high and ambient pCO_2, was enhanced via heterotrophic feeding. A number of experimental and field studies have demonstrated (Langdon and Atkinson 2005; Holcomb et al. 2010) or suggested (Atkinson et al. 1995; Atkinson and Cuet 2008; Cohen and Holcomb 2009; Shamberger et al. 2011; Edmunds 2011) that elevated dissolved inorganic nutrients (DIN) and/or nutrition via heterotrophic feeding could reduce the impact of elevated CO_2 on calcification. We chose to manipulate heterotrophic feeding conditions because the addition of DIN to coral cultures under ambient CO_2 can lead to decreased calcification due to a proposed disruption in the coral-zooxanthellae symbiosis (Muscatine et al. 1989; Falkowski et al. 1993; Marubini and Davis 1996), whereas heterotrophic feeding tends to enhance calcification under ambient CO_2 conditions (Houlbrèque and Ferrier-Pagès 2009).

Materials and Methods

Experimental Set-Up and Conditions

This experiment was conducted at the Bermuda Institute of Ocean Sciences (BIOS) in St. George's, Bermuda. The experimental treatments were two CO_2 levels (high and ambient) and two feeding conditions (fed and unfed). The two pCO_2 levels were established in static 5.5 gallon aquaria filled with serially filtered (50, 5 μm) seawater prior to the addition of metamorphosed larvae. These conditions were achieved and maintained by directly bubbling air (in the ambient condition) or CO_2-enriched air (high CO_2 treatment) through micropore bubble ''wands'' fixed horizontally approximately 5 cm from the base of each aquarium. A pair of Aalborg mass flow controllers maintained the CO_2 concentration of the enriched treatment. The resultant average calculated pCO_2 for ambient and high CO_2 conditions were 421 ± 35 and 1,311 ± 76 μatm (mean ± SD), respectively, with corresponding average Ωar of 3.66 ± 0.15 and 1.63 ± 0.08 (mean ± SD), respectively (Table 1). Ωar of our high CO_2 treatments is within range of average global surface ocean Ωar predicted by global climate models for the end of this century under the IPCC SRES

A2 (Steinacher et al. 2009). Corals in fed treatments were isolated (every night for 2 weeks, every other night for the third week) for 3 h in 12.5 cm x 12.5 cm x 3 cm plastic containers filled with seawater from their respective treatment tanks and provided with 24-h-old *Artemia* nauplii (brine shrimp). Feeding took place at night, shortly after lights were switched off to mimic crepuscular feeding and temporal zooplankton abundance observed in local coral reef environments (Lewis and Price 1975). Unfed corals were not provided nauplii during the 3-week experiment and were not isolated in empty feeding containers.

Each CO_2-feeding treatment was conducted in triplicate for a total of twelve aquaria, and all treatments were kept on a 12/12 h light–dark cycle. Fluorescent aquarium lamps maintained maximum light levels of 62 ± 8 μmol quanta m^{-2} s^{-1} (mean ± SD), which were monitored using a LI-COR probe/meter assemblage. The compensation range for *F. fragum* spat on Bermuda is not yet known. We used the low end of known compensation ranges for corals (e.g. 3–233 μmol quanta m^{-2} s^{-1} as reported by Mass et al. 2007) for two reasons. The first was to ensure that corals under elevated CO_2 did not bleach (as experienced by Anthony et al. 2009), and the second was to minimize the potential for enhanced photosynthesis to overwhelm or inhibit the feeding-modulated calcification response to elevated CO_2. Aquarium temperatures were maintained by in-line chiller/heater systems and monitored every 15 min (Hobo temperature loggers, Onset Corp.). Average temperature for all treatments over the course of the experiment was 27.6 ± 0.1 ^{o}C (± SD).

Aquarium water was replaced with filtered seawater every week to prevent the build-up of dissolved inorganic nitrogen and other wastes. Prior to removing water from the aquaria, we collected discrete water samples for salinity, alkalinity (Alk), and dissolved inorganic carbon (DIC) from every aquarium. Salinity was measured at BIOS with an Autosal salinometer. The Alk/DIC samples were poisoned with mercuric chloride immediately after collection and analyzed using a Marianda VINDTA-3C analysis system at WHOI. Alkalinity was determined by nonlinear curve fitting of data obtained by open-cell titrations, and DIC concentrations were determined by coulometric analysis. Both measurements were standardized using certified reference materials obtained from Dr. A. Dickson (Scripps IO). The pH (NBS) of each tank was measured every 3–4 d (Orion pH meter and temperature-compensated electrode) to provide a real-time assessment of tank chemistry. Short-term variations in NBS pH were also assessed on a higher-resolution time scale: for one, 24-h period, by measuring pH in each aquarium at 3-h time intervals. The pH within each tank was maintained within ± a few hundredths of a pH unit on both sub-weekly and sub-daily time scales. The carbonate system parameters used to compare treatments (pCO_2, $[HCO_3^-]$, $[CO_3^{2-}]$, and Ωar) were calculated from the average temperature and discretely sampled salinity, Alk, and DIC data using the CO2SYS program (Lewis and Wallace 1998; Pelletier et al. 2007) with the constants of Mehrbach et al. (1973) as refit by Dickson and Millero (1987) (Table 1).

Coral collection, spawning and larval settlement

In July 2010, approximately 1 week prior to anticipated peak larval release date (Goodbody-Gringley and de Putron 2009), we collected 30 mature colonies of the brooding coral, *F. fragum*, from the Bailey's Bay patch reefs off the northwest Bermudan coast at approximately three to seven meters water depth. Adult colonies were maintained in outdoor flow-through seawater aquaria at BIOS under ambient light and temperature conditions. Parent colonies were kept isolated in glass jars during planula release, which occurred over the course of 6 nights. The live zooxanthellate planulae were collected from all parents and pooled together. Ceramic tiles, approximately 9 cm^2, were left out on the reef for 2 months prior to the start of the experiment and further conditioned for larval settlement by scattering bits of freshly collected crustose coralline

algae on the tiles. Immediately after collection, actively swimming larvae were transferred to small plastic tubs each containing ceramic tiles and filled with seawater preset to targeted CO2 levels. The tubs had mesh lids, allowing for water exchange, while they are submerged in the treatment aquaria. After 48 h, larvae had settled and metamorphosed into primary polyps (at this stage, larvae are ‘‘spat’’). Spat on tiles were quickly counted, and tiles were pseudo-randomly distributed among the experimental aquaria so that each aquarium had approximately the same number of juvenile corals. Calcification was visible approximately 3 d after settlement. At the end of 3 weeks (± 1 d), 20–50 primary polyps (including their primary corallite) per treatment were removed from the tiles and frozen at -80 ^{o}C for analysis of total lipid. Tiles were then removed from treatments and submerged in a 10 % bleach solution for 1 h, which removed the polyp tissue from all of the remaining juvenile corals and exposed the calcified skeleton or primary corallite.

Quantification of skeletal development, size and weight

Each bleached skeleton was digitally photographed, removed from the tile, and weighed using a Metro-Toledo microbalance (Cohen et al. 2009; de Putron et al. 2011). Images of the spat were examined for skeletal development and size using Spot Imaging software. Length of the primary septa (present in all samples) was used to estimate corallite diameter (i.e., size). The septa are lateral CaCO3 plates that corals accrete in cycles (Fig. 1). In our experiment, most spat accreted both primary and secondary septa; the tertiary septa were the last septal cycle accreted by any of the juvenile corals. Rate of skeletal development was defined as percent spat exhibiting tertiary septa, and a two-way ANOVA was used to test for differences in the mean proportion of spat with tertiary septa between the treatments. Feeding treatment and CO_2 level were fixed effects (Electronic Supplemental Material, ESM Table S1). Data were arc sin square root transformed to homogenize variances prior to analyses.

To test for differences in mean spat weight and diameter among treatments, a two-way, nested multivariate analysis of variance (MANOVA) was performed on natural log transformed weight data and square root transformed diameter data. Feeding treatment and CO_2 levels were fixed main effects, while tank effect was the random factor nested within feeding and CO_2 levels (ESM Table S2). Eight univariate F tests were conducted to test each of the dependent variables. A Bonferonni corrected alpha value of 0.0062 was used to declare significance of F statistics (ESM Table S3). It should be noted that the MANOVA only considers corals that have data for both diameter and weight. If part of a corallite is lost during weighing or was attached to coralline algae, both coral size and weight were excluded from the MANOVA analyses. Likewise, if the skeleton was irregularly shaped (i.e., primary septa did not lie in a straight line), the data for those corals were not included. In order to account for any bias that may have resulted from corallite exclusion in the MANOVA, ANOVAs for the dependent variables, weight, and diameter were conducted. These tests considered all data for a given dependent variable to compare with the MANOVA’s univariate results.

Quantification of total lipid and symbiont density

Ten individual spat from each aquarium were pooled per tissue lipid sample for quantification of total lipid by gravimetric analysis. Pooling was necessary due to the small size of the spat at 3 weeks. Extraction methods follow that of Folch et al. (1957) and Cantin et al. (2007).

Five individual spat from each aquarium were pooled per sample for quantification of symbiont density. Spat were homogenized, centrifuged and the resultant pellet was re-suspended in 250 μL filtered seawater. Symbionts from multiple (6–9) aliquot sub-samples of the slurry were

counted on a known volume hemocytometer grid. Both total tissue lipid and symbiont counts were normalized to the circular area described by the average primary septa length (diameter) for a respective tank and then divided by the number of corals pooled in the sample (i.e., 10 or 5).

Both area-normalized lipid content and symbiont density were compared among levels of CO_2 and feeding conditions using two-way ANOVAs with tank as a random factor nested within the CO_2 and feeding combinations. Total lipid concentration was transformed to - 1/x in order to homogenize the variances. All statistical analyses were conducted on SYSTAT.

Results

Skeletal development

A significantly higher mean percentage of fed spat accreted tertiary septa (i.e., exhibited a faster rate of development) than did unfed spat (two-way ANOVA $p < 0.001$; ESM Table S1), but the percentage with tertiary septa did not differ between ambient and high CO_2 nor was there a significant interaction between CO_2 and feeding (Fig. 2 a; ESM Table S1).

Skeletal Size and Weight

Multivariate analysis (MANOVA) of both skeletal weight and diameter indicated that the effect due to CO_2 (ambient vs. high) and feeding treatments (fed vs. unfed) were both significant ($p < 0.001$; ESM Table S2), but the interaction between feeding and CO_2 was not significant. Univariate analyses of the effect of feeding indicate a significant impact on both corallite diameter and weight ($p < 0.001$; ESM Table S3): fed spat accreted larger and heavier skeletons. Likewise, CO_2 level significantly impacted corallite weight ($p < 0.001$; ESM Table S3): Skeletons accreted at ambient CO_2 were heavier than those raised under high CO_2 conditions for a given feeding regime. In contrast, the impact of CO_2 on skeletal diameter was not significant (ESM Table S3). The follow-up, independent ANOVAs for weight and diameter, conducted to account for potential bias due to corallite exclusion from the MANOVA, were consistent with the MANOVA's univariate results: Elevated CO_2 did not significantly impact the diameter (size) of the skeletons (Figs. 2 a, 3a) but did impact skeletal weight (Figs. 2 b, 3 b).

Lipid and symbiont density

We did not detect statistically significant differences in area-normalized zooxanthellae density and total tissue lipid content between fed and unfed spat or between CO_2 treatments (Fig. 4 a, b; ESM Table S4). There was significant variability among tanks, which reduced the power to detect differences between CO_2 and feeding treatments.

Discussion

Skeletal size and development, rate of $CaCO_3$ production, and energetic status (e.g., total lipid stores and metabolic performance) are key physiological indices of coral health and fitness. High growth rate contributes to juvenile coral survival and successful reef recruitment (Rylaarsdam 1983; Hughes and Jackson 1985; Vermeij and Sandin 2008). Linear extension affects a colony's ability to compete for space with algae and reduced skeletal density may affect the structural integrity of the coral holobiont (Hoegh-Guldberg et al. 2007). Further, energetic reserves

have been used to model and predict coral colony mortality risk (Anthony et al. 2009). These parameters are sensitive to a number of environmental stressors. For example, skeletal growth and calcification tend to decline in corals stressed by elevated temperatures (e.g., Rodrigues and Grottoli 2006; Cooper et al. 2008; Cantin et al. 2010) or eutrophication (Marubini and Atkinson 1999), and bleaching can result in rapid depletion of energetic reserves (e.g., Grottoli et al. 2004; Rodrigues and Grottoli 2007). Given anticipated (Kleypas et al. 1999) and experimentally observed (e.g., Langdon and Atkinson 2005) declines in coral calcification due to acidification, it has been suggested that OA may increase the energetic demands of $CaCO_3$ production (Cohen and Holcomb 2009 Holcomb et al. 2010; Ries 2011).

In this study, OA induced by significantly elevated levels of CO_2 had no effect on the rate of development of septal cycles and skeletal diameter (size) nor could we detect a significant effect on area-normalized total tissue lipid content and symbiont density of juvenile corals reared from planulae larvae (Figs. 2, 4). Conversely, fed juveniles reared under elevated CO_2 conditions (~ 5 times preindustrial) exhibited faster tertiary septa development and had larger skeletons than unfed juveniles reared under ambient CO2 levels (~ 1.5 times preindustrial). Thus, for newly settled corals of this species, OA may have little, if any, impact on lateral size and septal development, whereas factors that impact food availability or a coral's ability to acquire food could affect these aspects of postsettlement growth.

Heterotrophic feeding also significantly impacted the rate of $CaCO_3$ production (as measured by total corallite weight). Under both ambient and elevated CO_2 conditions, fed corals produced significantly more $CaCO_3$ over the 3-week experimental period than unfed corals (Fig. 2 c). At 421 μatm CO_2, fed corals produced 55 % more $CaCO_3$ than unfed corals; at 1,311 μatm CO_2, the difference was 68%. Thus, under significantly elevated CO_2 conditions, fed spat develop faster, grow bigger, and weigh more than unfed spat. This suggests that, to the extent that young corals affect the reef $CaCO_3$ budget, nutritionally enhanced juveniles contribute more $CaCO_3$ than those that are nutritionally restricted and subjected to the same CO_2 conditions. Remarkably, fed juveniles subjected to significantly elevated CO_2 also develop faster and grow larger than unfed corals reared under ambient CO_2 conditions, and their rate of $CaCO_3$ production are comparable. Therefore, by implication, nutritionally replete corals could perform better under OA than corals that are nutritionally restricted.

Nevertheless, our results indicate that feeding does not mitigate the impact of OA on calcification by juvenile corals. In both fed and unfed groups, skeletal weight decreased, by 23.0 ± 2.9 and 28.9 ± 0.1 %, respectively (~ 8–14 % per unit drop in omega), under elevated CO_2. This change is equivalent to that observed by de Putron et al. (2011) for both acid addition and CO_2 manipulation experiments with the same Favia species, although it is significantly less than the 80 % drop predicted by the Langdon and Atkinson model (2005).

A number of studies report increased calcification by corals under heterotrophic feeding (e.g., Houlbrèque and Ferrier-Pagès 2009), which is consistent with the observations in this study. However, our data show that the negative effect of OA on calcification persists under conditions of heterotrophic feeding. In our study, feeding did not change the sensitivity of calcification to OA. This suggests that nutritional enhancement via heterotrophic feeding did not change the mechanics of the calcification response to OA in our corals. Although Edmunds (2011) concluded that heterotrophic feeding does mitigate the impact of elevated CO_2 on juvenile Porites calcification, both the fed and unfed Porites corals in his experiment exhibited reduced biomass-corrected calcification under elevated CO_2, which is consistent with our result for Favia. Indeed, Edmunds' (2011) result lends support to our observation that the sensitivity of calcification response to elevated CO_2 is consistent between fed and unfed corals. In other words, heterotrophic feeding

does not mitigate the effect of OA on coral calcification.

That heterotrophic feeding does not mitigate the impact of OA on juvenile coral differs from the results of Langdon and Atkinson (2005) and Holcomb et al. (2010) who reported significant modulation of the CO_2 effect with inorganic nutrient enrichment. In these studies, addition of ammonium, and of nitrates, phosphates, and iron, respectively, did reduce calcification sensitivity to OA. In the experiments of Langdon and Atkinson (2005), nutrient addition enhanced symbiont photosynthesis (photosynthesis was not measured in Holcomb et al. (2010). We were not able to detect a significant impact on area-normalized symbiont densities due to feeding in our experiments (Fig. 4b). This observation is different from that reported by a number of previous studies (Muscatine et al. 1989; Titlyanov et al. 2000a, b, 2001; Houlbrèque et al. 2003, 2004) and may be due to our lack of statistical power to detect a significant feeding effect. Alternatively, although our corals were fully zooxanthellate at the time of settlement, the impact of feeding on symbiont densities might differ between young corals and the mature colonies used in other experiments. Endosymbiont density is only one component of the coral holobiont's photosynthetic capacity and is not a substitute for direct measurements of photosynthesis (e.g., Langdon and Atkinson 2005) because the performance of individual symbionts is still unknown. Therefore, we can only speculate that the difference between our result (i.e., no significant difference detected in symbiont density or reduction in sensitivity to CO_2 due to feeding) and that of Langdon and Atkinson (2005), that is, DIN enrichment resulting in enhanced photosynthesis and reduced sensitivity to CO_2, suggest a role for symbiont photosynthesis in the coral calcification response to OA. From our data, it does not appear that simply enhancing coral energetic status (in this case, via feeding) alters calcification sensitivity to OA. However, photosynthesis and heterotrophy may impact coral calcification via different mechanisms. If this is the case, then the impact of OA on calcification when photosynthesis is enhanced might differ from the impact of OA on calcification when feeding is enhanced. Incidentally, it should be noted that the degree to which feeding impacted calcification rates in this study may be specific to our relatively low-light regime and test species and could therefore differ among organisms subjected to higher light environments.

Additionally, fast-growing, prereproductive juvenile corals might respond to feeding differently from adults, which were used in both the Langdon and Atkinson (2005) and Holcomb et al. (2010) experiments. Adult corals may allocate the extra energy from heterotrophic feeding differently from juveniles. To investigate whether our juvenile corals were storing the extra energy from heterotrophic feeding as lipid reserve, or using it to build new tissue or skeleton, we averaged total tissue lipid content over circular surface area (Fig. 4 b). We could not detect a significant difference in the amount of lipid accumulated by the corals in the different feeding regimes. This suggests that, in this particular experiment, the fed coral spat did not store the extra energy acquired from feeding but rather used it for growth. Whether or not mature colonies in experimental conditions and on actual reefs respond to food availability the same way, that is, by investing in tissue growth rather than lipid storage, is yet to be tested.

Our results show that healthy, nutritionally replete spat of the Atlantic coral, *F. fragum*, can sustain high rates of calcification under significantly elevated CO_2. However, enhanced nutritional status does not render these corals immune to OA. This has important implications for the ability of corals and coral reefs to maintain levels of growth and $CaCO_3$ production required to sustain reef ecosystems through increasingly hostile conditions over the twenty first century.

Acknowledgements

Acknowledgments The authors are grateful to Rebecca Belastock (WHOI) for DIC/Alk analyses.

We also thank Ms. Hannah Barkley (WHOI), Ms. Kascia White (BIOS) and Mr. Mark Dowar (BIOS) for assistance with fieldwork and experiment maintenance, and Dr Neal Cantin (WHOI) for assistance with laboratory procedures. This project was funded by NSF OCE-1041106 and NSF OCE-1041052, a WHOI winter intern fellowship to A. Zicht made possible by the A. V. Davis Foundation and support from the MIT/WHOI Bermuda Biological Station for Research Fund. We thank the three anonymous reviewers and the editor for suggestions that greatly improved the manuscript.

Reference List

Atkinson MJ, Cuet P (2008) Possible effects of ocean acidification on coral reef biogeochemistry: topics for research. Mar Ecol Prog Ser 373:249-256

Atkinson MJ, Carlson B, Crowe JB (1995) Coral growth in high-nutrient, low pH seawater: a case study in coral growth at the Waikiki aquarium. Coral Reefs 14: 215-233

Anthony KR, Hoogenboom MO, Maynard JA, Grottoli AG, Middlebrook R (2009) Energetics approach to predicting mortality risk from environmental stress: a case study of coral bleaching. Funct Ecol 23: 539-550

Caldeira K, Wickett ME (2003) Anthropogenic carbon and ocean pH. Nature 425: 365

Cantin NE, Negri AP, Willis BL (2007) Photoinhibition from chronic herbicide exposure reduces reproductive output of reef-building corals. Mar Ecol Prog Ser 344:81-93

Cantin NE, Cohen AL, Karnauskas KB, Tarrant AM, McCorkle DC (2010) Ocean warming slows coral growth in the central Red Sea. Science 329:322-325

Cohen AL, Holcomb M (2009) Why corals care about ocean acidification: uncovering the mechanism. Oceanography 22:118-127

Cohen AL, McCorkle DC, de Putron S, Gaetani GA, Rose KA (2009) Morphological and compositional changes in the skeletons of new coral recruits reared in acidified seawater: Insights into the biomineralization response to ocean acidification. Geochem Geophys Geosy 10:Q07005

Cooper TF, De'ath G, Fabricius KE, Lough JM (2008) Declining coral calcification in massive *Porites* in two nearshore regions of the northern Great Barrier Reef. Global Change Biol 14:529-538

de Putron SJ, McCorkle DC, Cohen AL, Dillon AB (2011) The impact of seawater saturation state and bicarbonate ion concentration on calcification by new recruits of two Atlantic corals. Coral Reefs 30:321-328

Dickson AG, Millero FJ (1987) A comparison of the equilibrium constants for the dissociation of carbonic acid in seawater media. Deep-Sea Res 34:1733–1743

Doney SC, Fabry VJ, Feely RA, Kleypas JA (2009) Ocean acidification: The other CO_2 problem. Annu Rev Mar Sci 1:169-192

Edmunds PJ (2011) Zooplanktivory ameliorates the affects of ocean acidification on the reef coral *Porites* spp. Limnol Oceanogr 56:2402-2410

Fabry VJ, Seibel BA, Feely RA, Orr JC (2008) Impacts of ocean acidification on marine fauna and ecosystem processes. ICES J Mar Sci 65:414–432

Falkowski PG, Dubinsky Z, Muscatine L, McCloskey L (1993) Population control in symbiotic corals. BioScience 42: 606-611

Feely RA, Sabine CL, Lee K, Berelson W, Kleypas J, Fabry VJ, Millero FJ (2004) Impact of anthropogenic CO_2 on the $CaCO_3$ system in the oceans. Science 305:362–366

Folch J, Lees M, Sloane Stanley GH (1957) A simple method for the isolation and purification of total lipids from animal tissue. J Biol Chem 226:497-509

Goodbody-Gringley G, de Putron SJ (2009) Planulation patterns of the brooding coral, *Favia fragum*, in Bermuda. Coral Reefs 28:959-963

Grottoli, AG, Rodrigues LJ, Juarez C (2004) Lipids and stable carbon isotopes in two species of Hawaiian corals, *Porites compressa* and *Montipora verrucosa*, following a bleaching event. Mar Biol 145: 621–631

Hoegh-Guldberg O, Mumby PJ, Hooten AJ, Steneck RS, Greenfield P, Gomez E, Harvell CD, Sale PF, Edwards AJ, Caldeira K, Knowlton N, Eakin CM, Iglesias-Prieto R, Muthiga N,

Bradbury RH, Dubi A, Hatziolos ME (2007) Coral reefs under rapid climate change and ocean acidification. Science 318:1737-1742

Holcomb M, McCorkle DC, Cohen AL (2010) Long-term effects of nutrient and CO_2 enrichment on the temperate coral *Astrangia poculata* (Ellis and Solander, 1786). J Exp Mar Biol Ecol 386:27-33

Houlbrèque F, Ferrier-Pagès C (2009) Heterotrophy in tropical scleractinian corals. Biol Rev Camb Philos Soc 84:1-17

Houlbrèque F, Tambutte E, Ferrier-Pages, C (2003) Effect of zooplankton availability on the rates of photosynthesis, and tissue and skeletal growth in the scleractinian coral *Stylophora pistillata*. J Exp Mar Biol Ecol 296: 145-166

Houlbrèque F, Tambutte E, Allemand D, Ferrier-Pages C (2004) Interactions between zooplankton feeding, photosynthesis and skeletal growth in the scleractinian coral *Stylophora pistillata*. 207: 1461-1469

Hughes TP, Jackson JBC (1985) Population-dynamics and life histories of foliaceous corals. Ecol Monogr 55:141-166

Kleypas J, Buddemeier R, Archer D, Gattuso J, Langdon C, Opdyke B (1999) Geochemical consequences of increased atmospheric carbon dioxide on coral reefs. Science 284:118-120

Langdon C, Atkinson MJ (2005) Effect of elevated pCO_2 on photosynthesis and calcification of corals and interactions with seasonal change in temperature/irradiance and nutrient enrichment. J Geophys Res-Oceans 110:1-54

Langdon C, Takahashi T, Sweeney C, Chipman D, Goddard J, Marubini F, Aceves H, Barnett H, Atkinson MJ (2000) Effect of calcium carbonate saturation state on the calcification rate of an experimental coral reef. Global Biogeochem Cycles 14: 639-654

Lewis E, Wallace DWR (1998) Program developed for CO_2 system calculations. ORNL/CDIAC-105, Carbon Dioxide Information Analysis Center Oak Ridge Natl Lab. US Dept of Energy, Oak Ridge, TN

Lewis JB, Price WS (1975) Feeding mechanisms and feeding strategies of Atlantic reef corals. J Zool 176:527-544

Marubini F, Davies PS (1996) Nitrate increases zooxanthellae population density and reduces skeletogenesis in corals. Mar Biol 127:319-328

Marubini F, Atkinson MJ (1999) Effects of lowered pH and elevated nitrate on coral calcification. Mar Ecol Prog Ser 188:117-121

Mass T, Einbinder S, Brokovich E, Shashar N, Vago R, Erez J, Dubinsky Z (2007) Photoacclimation of *Stylophora pistillata* to light extremes: metabolism and calcification. Mar Ecol Prog Ser 334:93-102

Mehrbach C, Culberso CH, Hawley JE, Pytkowic RM (1973) Measurement of apparent dissociation-constants of carbonic-acid in seawater at atmospheric-pressure. Limnol Oceanogr 18:897–907

Mucci A (1983) The solubility of calcite and aragonite in seawater at various salinities, temperatures, and one atmosphere total pressure. Am J Sci 283:780-799

Muscatine L, Falkowski PG, Dubinsky Z, Cook PA, McCloskey LR (1989) The effect of external nutrient resources on the population-dynamics of zooxanthellae in a reef coral. Proc R Soc B-Biol Sci 236:311-324

Orr JC, Fabry VJ, Aumont O, Bopp L, Doney SC, Feely RA, Gnanadesikan A, Gruber N, Ishida A, Joos F, Key RM, Lindsay K, Maier-Reimer E, Matear R, Monfray P, Mouchet A, Najjar RG, Plattner GK, Rodgers KB, Sabine CL, Sarmiento JL, Schlitzer R, Slater RD, Totterdell

IJ, Weirig MF, Yamanaka Y, Yool A (2005) Anthropogenic ocean acidification over the twenty-first century and its impact on calcifying organisms. Nature 437: 681-686
Pandolfi JM, Connolly SR, Marshall DJ, Cohen AL (2011) Projecting coral reef futures under global warming and ocean acidification. Science 333:418-422
Pelletier G, Lewis E, Wallace D (2007) CO2sys.xls: A Calculator for the CO_2 System in Seawater for Microsoft Excel/VBA. Washington State Department of Ecology/Brookhaven National Laboratory, Olympia, WA/Upton, NY, USA
Ries JB (2011) A physicochemical framework for interpreting the biological calcification response to CO2-induced ocean acidification. Geochim Cosmochim Acta 75: 4053-4064
Ries JB, Cohen AL, McCorkle DC (2010) A nonlinear calcification response to CO_2-induced ocean acidification by the coral *Oculina arbuscula*. Coral Reefs 29:661-674
Rodrigues LJ, Grottoli AG (2006) Calcification rate and the stable carbon, oxygen, and nitrogen isotopes in the skeleton, host tissue, and zooxanthellae of bleached and recovering Hawaiian corals. Geochim Cosmochim Acta 70:2781-2789
Rodrigues LJ, Grottoli A (2007) Energy reserves and metabolism as indicators of coral recovery from bleaching. Limnol Oceanogr 52:1874-1882
Rylaarsdam KW (1983) Life histories and abundance patterns of colonial corals on Jamaican reefs. Mar Ecol Prog Ser 13:249-260
Shamberger KEF, Feely RA, Sabine CL, Atkinson MJ, DeCarlo EH, Mackenzie FT, Drupp PS, Butterfield DA (2011) Calcification and organic production on a Hawaiian coral reef. Mar Chem 127:64-75
Silverman J, Lazar B, Erez J (2007) Community metabolism of a coral reef exposed to naturally varying dissolved inorganic nutrient loads. Biogeochemistry 84:67-82
Silverman J, Lazar B, Cao L, Caldeira K, Erez J (2009) Coral reefs may start dissolving when atmospheric CO_2 doubles. Geophys Res Lett 26:1-5
Steinacher M, Joos F, Frölicher TL, Plattner G-K, Doney SC (2009) Imminent ocean acidification in the Arctic projected with the NCAR global coupled carbon cycle-climate model. Biogeosciences, 6, 515-533, doi:10.5194/bg-6-515-2009
Titlyanov EA, Titlyanova TV, Yamazato K, van Woesik R (2001) Photo-acclimation of the hermatypic coral *Stylophora pistillata* while subjected to either starvation or food provisioning. J Exp Mar Biol Ecol 257:163-181
Titlyanov EA, Tsukahara J, Titlyanova TV, Leletkin VA, van Woesik R, Yamazato K(2000b) Zooxanthellae population density and physiological state of the coral *Stylophora pistillata* during starvation and osmotic shock. Symbiosis 28:303-322.
Titlyanov E, Bil' K, Fomina I, Titlyanova T, Leletkin V, Eden N, Malkin A, Dubinsky Z (2000a) Effects of dissolved ammonium addition and host feeding with *Artemia salina* on photoacclimation of the hermatypic coral *Stylophora pistillata*. Mar Biol 127:319-328
Vermeij MJA, Sandin SA (2008) Density-dependent settlement and mortality structure the earliest life phases of a coral population. Ecology 89:1994-2004

Figure Legends

Figure 1. Three-week-old *F. fragum* corallites from (a) fed corals and (b) unfed corals in this study. In both images, the different septal stages are identified. Primary septa are indicated with green arrows, secondary with blue, and tertiary with red. White lines along the primary septa in (a) indicate corallite diameter used to determine lateral size. Scale bars are 1 mm

Figure 2. The percent of spat in a given treatment exhibiting tertiary septa (a), the diameter of primary septa (b), and the corallite weight (c) of fed and unfed spat. Bars indicate the average across three replicate tanks, which are themselves averaged across the number of samples for a given tank. Gray bars indicate high CO_2 and white bars indicate ambient CO_2 conditions. Error bars represent ± one standard error among replicate tanks

Figure 3. Corallite diameter (a) and total corallite weight (b) versus Ωar observed in fed (filled diamonds) and unfed (empty diamonds) corals. Error bars represent ± one standard error for replicate analyses of each tank

Figure 4. Area-normalized total tissue lipid weight per spat in fed and unfed corals. Bars indicate the average across three replicate tanks, which are themselves averaged across the number of samples for a given tank. Gray bars indicate high CO_2 and white bars indicate ambient CO_2 conditions. Error bars represent ± one standard error among replicate tanks. Although these plots depict the raw data from the experiment, the ANOVA was performed on the transformed data, which met the criteria for homogeneity of variance

Table 1. Measurements and calculations of experimental carbonate and seawater chemistry conditions Average (±SD) seawater chemistry for given experimental treatment conditions. Average temperature (27.6 ^{o}C) and measured salinity, alkalinity, and DIC were used to calculate pCO_2, pH, $[HCO_3^-]$, $[CO_3^{2-}]$, and aragonite saturation state (Ωar) for each aquarium using CO2SYS (Lewis and Wallace 1998). We used Dickson and Millero's (1987) dissociation constants from the refit of Mehrbach et al. (1973) and the aragonite solubility of Mucci (1983). We computed mean treatment condition from the average values of each treatment's three replicate tanks. One anomalous pair of alkalinity/DIC values from one aquarium was omitted from the calculations for the ambient, fed aquaria.

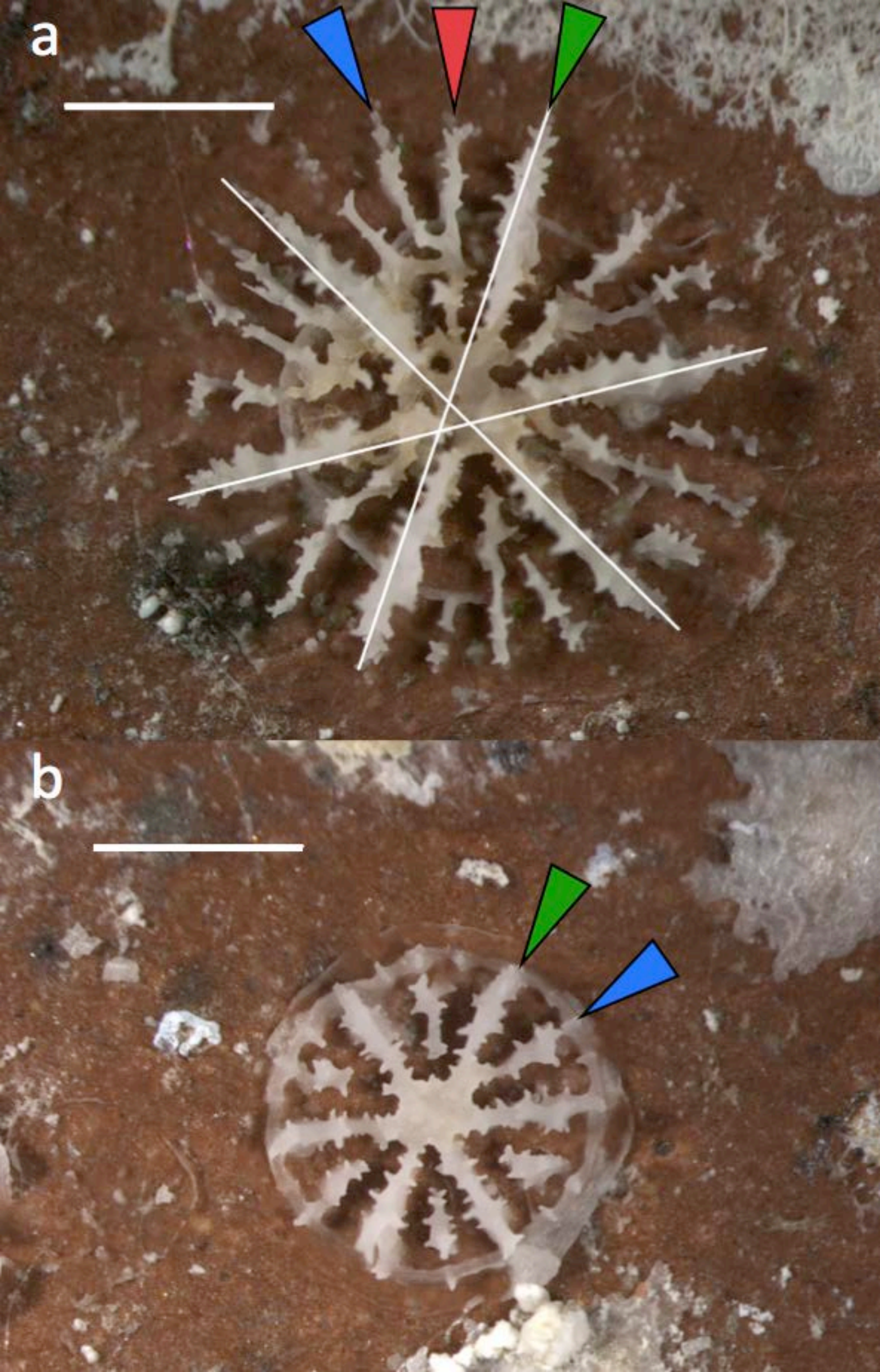
a
b

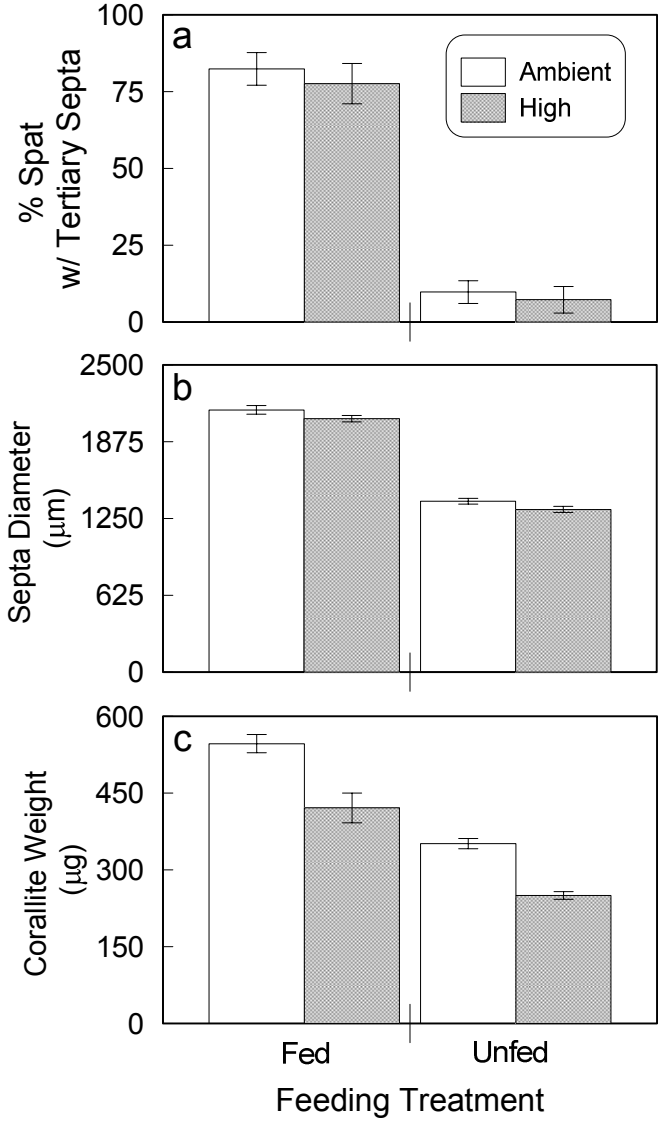
a
b
c
Ambient
High
% Spat w/ Tertiary Septa
Septa Diameter (μm)
Corallite Weight (μg)
100
75
50
25
0
2500
1875
1250
625
0
600
450
300
150
0
Fed
Unfed
Feeding Treatment

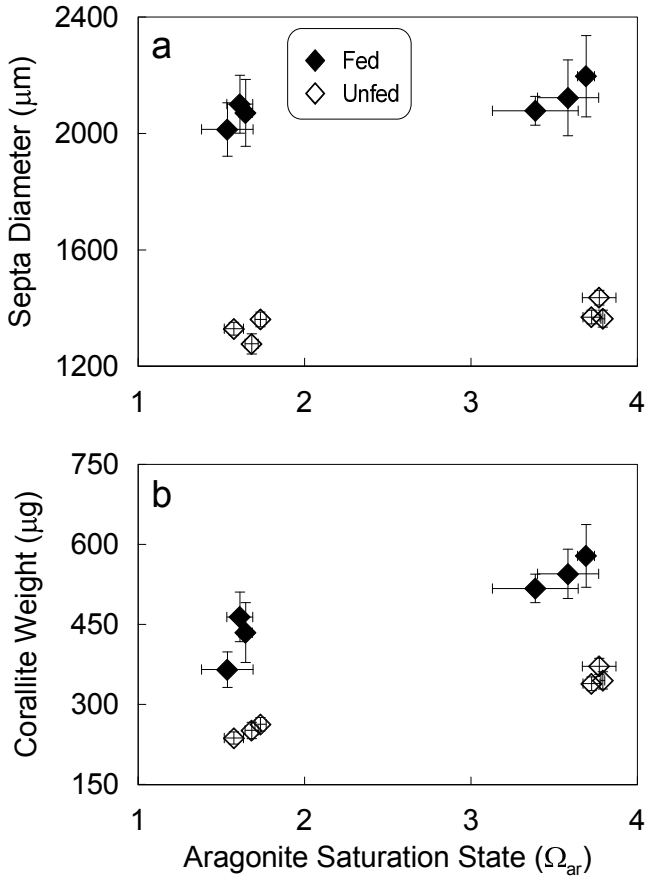
a
Fed
Unfed
Septa Diameter (μm)
2400
2000
1600
1200
1
2
3
4
b
Corallite Weight (μg)
750
600
450
300
150
Aragonite Saturation State (Ωar)

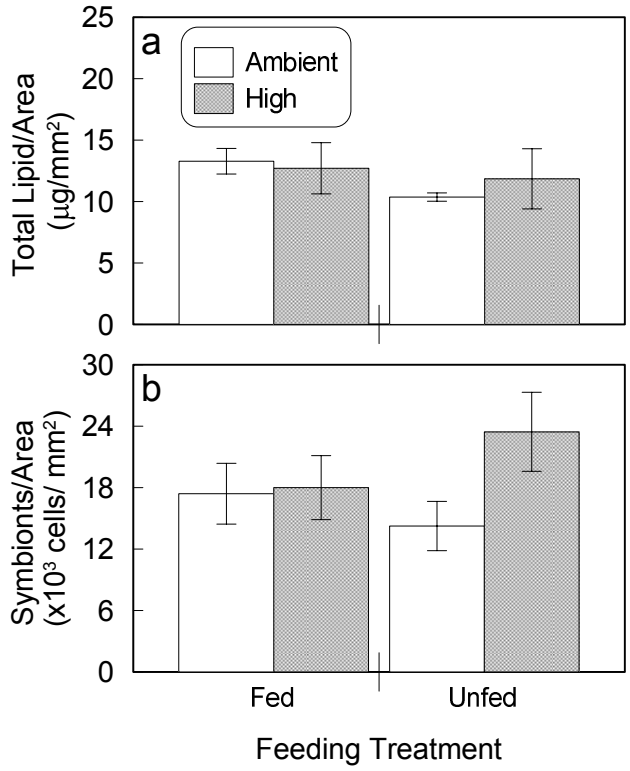
a
Ambient
High
Total Lipid/Area
(µg/mm²)
25
20
15
10
5
0
b
Symbionts/Area
(x10³ cells/ mm²)
30
24
18
12
6
0
Fed
Unfed
Feeding Treatment

Table 1. Measurements and calculations of experimental carbonate and seawater chemistry conditions
Average (± SD) seawater chemistry for given experimental treatment conditions. Average temperature (27.6°C) and measured salinity, alkalinity, and DIC were used to calculate pCO_2, pH, $[HCO_3^-]$, $[CO_3^{2-}]$ and aragonite saturation state (Ω_{ar}) for each aquarium using CO_2SYS (Lewis and Wallace, 1998). We used Dickson and Millero's (1987) dissociation constants from the refit of Mehrbach *et al* (1973) and the aragonite solubility of Mucci (1983). We computed mean treatment condition from the average values of each treatment's three replicate tanks. One anomalous pair of alkalinity/DIC values from one aquarium was omitted for the calculations for the Ambient, Fed aquaria.

Treatment	**Salinity (psu ± SD)**	**Alkalinity (ueq/kg ± SD)**	**DIC (µmol/kg ± SD)**	**pCO_2 (µatm ± SD)**	**pH (Total ± SD)**	**$[HCO_3^-]$ (µmol/kg ± SD)**	**$[CO_3^{2-}]$ (µmol/kg ± SD)**	**Ω_{ar} (± SD)**
Ambient CO_2, Fed	37.6 ± 0.3	2332 ± 22	2012 ± 33	443 ± 40	8.00 ± 0.03	1775 ± 40	225 ± 9	3.55 ± 0.16
Ambient CO_2, Unfed	37.4 ± 0.3	2325 ± 20	1984 ± 16	398 ± 4	8.04 ± 0.00	1735 ± 13	239 ± 3	3.77 ± 0.03
High CO_2, Fed	37.0 ± 0.2	2324 ± 9	2213 ± 16	1344 ± 78	7.59 ± 0.02	2077 ± 17	100 ± 4	1.59 ± 0.06
High CO_2, Unfed	37.0 ± 0.2	2326 ± 23	2207 ± 21	1278 ± 70	7.61 ± 0.02	2069 ± 20	105 ± 5	1.66 ± 0.08